



## Theoretical analysis and experimental study on metal separation of tungsten-containing systems



Liwen Ma<sup>a,b</sup>, Xiaoli Xi<sup>a,b,\*</sup>, Zhiqiang Huang<sup>a</sup>, Zuoren Nie<sup>a,b</sup>

<sup>a</sup> College of Materials Science and Engineering, Beijing University of Technology, Beijing 100124, China

<sup>b</sup> National Engineering Laboratory for Industrial Big-data Application Technology, Beijing University of Technology, Beijing 100124, China

### ARTICLE INFO

#### Keywords:

Tungsten-containing system  
Metal separation  
E-pH diagram  
Orthogonal experiment

### ABSTRACT

Based on the leaching solution of tungsten secondary resource, the metal separation properties of tungsten-containing systems such as the W-Mg-Si-H<sub>2</sub>O, the W-Al-H<sub>2</sub>O, the W-Fe-Mo-H<sub>2</sub>O and the W-Ca-V-H<sub>2</sub>O, were investigated by theoretical E-pH diagrams and experiments. The results demonstrated that the precipitation rates of Si and W were 99% and 2.4% respectively at pH = 9 in W-Mg-Si-H<sub>2</sub>O system; the precipitation rates of Al and W were 99.8% and 3.0% respectively at pH = 7 in W-Al-H<sub>2</sub>O system; the precipitation rates of W and Mo were 95% and 24% respectively at pH = 7 in W-Fe-Mo-H<sub>2</sub>O system; the precipitation rates of V and W were 91.2% and 4.3% respectively at pH = 13 with Ca:V = 3:1 in V-Ca-W-H<sub>2</sub>O system. The theoretical predictions were in good agreement with the experimental results. The metal separation for a tungsten-containing polymetallic solution of W, Mo, V, Si and Al, was designed and the parameters were optimized through the orthogonal experiments. The metals of (Si/Al), V, W and Mo were separated step by step with the precipitation rates exceeding 92%. This study provided a reference to metal comprehensive separation and recovery for the tungsten secondary resources.

### 1. Introduction

Tungsten, as a rare metal, with high melting point, high specific gravity and high hardness, is an irreplaceable strategic resource and widely utilized in aerospace, atomic energy, shipbuilding, as well as in the automobile, the electronics and the chemical industries. The use and waste of tungsten is yearly increasing [1]. If the abandoned tungsten is not properly recovered, it will cause pollution to the environment and a waste of resources [2,3]. At present, the recovery researches of tungsten secondary resource are focused on the recycling methods for several typical wastes. As an example, the recovery process of tungsten slag or alloy scrap is to roast the wastes and the other materials, such as sodium carbonate, sodium sulfate, sodium nitrate, sodium hydroxide, quartz and sodium chloride, all consequently being leached to obtain soluble Na<sub>2</sub>WO<sub>4</sub> with water. The leaching solution is purified following ammonia is added to obtain ammonium paratungstate (APT). Finally, calcination and reduction follow, to obtain pure tungsten [4–8]. The recovery methods of the carbide waste are divided into two categories; one category is the selective Co extraction, leaving tungsten carbide WC. This is achieved through the acid leaching method, the high temperature treatment method, the zinc melting method or the selective electrochemical dissolution method. The other category is the

complete destruction of the alloy structure through a complete smelting process to recover tungsten [9–14].

The metal elements in typical tungsten secondary resources are presented in Table 1 [4–6,8,14]. During the tungsten secondary resource recovery process, the alkali leaching solution might contain the main elements of W, V, Mo, Al and Si, as Fe, Mn, Cu, Co and Ni in alkaline solution are easy to form precipitates and Ti is not easy to be leached. The separation of these metallic ions from the tungsten-containing leaching solution is one of the core aspects of the recovery process. The quantity of regenerated tungsten strongly lies in the purity. The higher the purity is, the lower the defects of the product are, whereas the better the performance of the material during the service is. At present, the metal separation methods for tungsten solution are the precipitation [15–17], the solvent extraction [18,19] and the ion exchange [20,21]. The separation methods are different depending on the types of metals in the tungsten solution. For certain impurity metals which are difficult to be dealt with, the removal methods are mainly the ion exchange or the solvent extraction method. However, the ion exchange method or solvent extraction method has the disadvantage of excessive investment. As an example, the overall investment in the ion exchange production line accounts for 1/3 of the entire investment and the actual ion exchange production costs accounts for 40% of the entire

\* Corresponding author at: College of Materials Science and Engineering, Beijing University of Technology, Beijing 100124, China.

E-mail address: [xixiaoli@bjut.edu.cn](mailto:xixiaoli@bjut.edu.cn) (X. Xi).

<https://doi.org/10.1016/j.seppur.2018.07.013>

Received 9 February 2018; Received in revised form 28 June 2018; Accepted 6 July 2018

Available online 07 July 2018

1383-5866/ © 2018 Elsevier B.V. All rights reserved.

**Table 1**  
Types of metal elements in tungsten secondary resources [4–6,8,14].

Waste type	Metal element
Tungsten slag	Si, W, Fe, Mn, Cu, Mo
Waste SCR catalyst	Ti, Si, W, Al, Ca, V, Fe, Mg, Mo
Tungsten alloy scraps	W, Si, V, Al
Hardmetal sludge	W, Co, Fe, Si, Ni

production costs. In addition, the solvent extraction also has the disadvantage of bad working environment because the reagents are usually organic compounds with volatility and certain toxicity. The precipitation method for metal separation is conducive to the industrial production with relatively low input and rapid output, however, the disadvantage is the relatively low purity for production. Therefore, it is of high significance to conduct a theoretical analysis, an experimental study and a process design of various metal precipitation separations of the tungsten-containing systems for the comprehensive recovery of tungsten secondary resources.

In this paper, based on the tungsten leaching solution, the E-pH diagrams of the tungsten-containing systems, such as the W-Mg-Si-H<sub>2</sub>O, the W-Al-H<sub>2</sub>O, the W-Fe-Mo-H<sub>2</sub>O and the W-Ca-V-H<sub>2</sub>O, were plotted and analyzed. The metal separation properties of these systems were studied by simulation solution. Finally, the metal separation process for a tungsten-containing polymetallic solution of W, Mo, V, Si and Al, was designed and the parameters were optimized through orthogonal experiments.

## 2. Experimental procedures

### 2.1. E-pH diagram of tungsten-containing systems

The E-pH diagrams of tungsten-containing systems such as the W-Mg-Si-H<sub>2</sub>O, the W-Al-H<sub>2</sub>O, the W-Fe-Mo-H<sub>2</sub>O and the W-Ca-V-H<sub>2</sub>O were plotted through HSC Chemistry 6.0 software. The conditions of the E-pH diagrams of W-Mg-Si-H<sub>2</sub>O system were as follows: [Mg]<sub>T</sub> = 0.1 mol/L, [W]<sub>T</sub> = 0.1 mol/L and [Si]<sub>T</sub> = 0.1 mol/L, pH = 0–14. The conditions of the E-pH diagram of the W-Al-H<sub>2</sub>O system were as follows: [W]<sub>T</sub> = 0.1 mol/L and [Al]<sub>T</sub> = 0.01 mol/L, pH = 0–14. The conditions of the E-pH diagrams of W-Fe-Mo-H<sub>2</sub>O system were as follows: [W]<sub>T</sub> = 0.1 mol/L, [Fe]<sub>T</sub> = [Mn]<sub>T</sub> = 0.1 mol/L and [Mo]<sub>T</sub> = 0.1 mol/L, pH = 0–14. The conditions of the E-pH diagrams of the W-Ca-V-H<sub>2</sub>O system were as follows: [W]<sub>T</sub> = 0.1 mol/L, [Ca]<sub>T</sub> = 0.15 mol/L and [V]<sub>T</sub> = 0.1 mol/L, pH = 0–18.

### 2.2. Precipitation separation of tungsten-containing systems

The W-Mg-Si-H<sub>2</sub>O solution was prepared by the mixing and stirring of sodium silicate along with sodium tungstate and pure water, where  $C_{Na_2WO_4} = C_{Na_2SiO_3} = 0.1$  mol/L. Following, the mixed solution was bathed at 25 °C for 30 min. Consequently, the MgCl<sub>2</sub> solution was slowly added, with a drop speed of 0.2 mL/min and a stirring speed of 300 r/min,  $C_{MgCl_2} = 0.1$  mol/L, whereas the sulfuric acid and sodium hydroxide were utilized to adjust the pH to 7–10. The precipitation rate was studied at different times.

The W-Al-H<sub>2</sub>O solution was prepared by the mixing and stirring of aluminum nitrate along with sodium tungstate and pure water, where  $C_{Na_2WO_4} = 0.1$  mol/L and  $C_{Al(NO_3)_3} = 0.01$  mol/L. Following, the mixed solution was bathed at 25 °C for 30 min with a drop speed of 0.2 mL/min and a stirring speed of 300 r/min, whereas the sulfuric acid and the sodium hydroxide were utilized to adjust the pH to 6–8. The precipitation rate was studied at different times.

The W-Fe-Mo-H<sub>2</sub>O solution was prepared by the mixing and stirring of sodium molybdate along with sodium tungstate and pure water, where  $C_{Na_2WO_4} = C_{Na_2MoO_4} = 0.1$  mol/L. Following, the mixed solution

was bathed at 25 °C for 30 min. Consequently, the FeSO<sub>4</sub> solution was slowly added, with a drop speed of 0.2 mL/min and a stirring speed of 300 r/min,  $C_{FeSO_4} = 0.1$  mol/L, whereas the sulfuric acid and the sodium hydroxide were utilized to adjust the pH to 7–10. The precipitation rate was studied at different times.

The W-Ca-V-H<sub>2</sub>O solution was prepared by the mixing and stirring of sodium vanadate along with sodium tungstate and pure water, where  $C_{Na_2WO_4} = C_{NaVO_3} = 0.01$  mol/L. Following, the mixed solution was bathed at 25 °C for 30 min. Consequently, the Ca(OH)<sub>2</sub> solution was slowly added, with a drop speed of 0.2 mL/min and a stirring speed of 300 r/min,  $C_{Ca(OH)_2} = 0.015$  mol/L, whereas the sulfuric acid and the sodium hydroxide were utilized to adjust the pH to 13. The precipitation rate was studied at different time. The effect of molar ratio of Ca(OH)<sub>2</sub> and NaVO<sub>3</sub> (Ca:V) on precipitation rate was studied at 25 °C for 2 h when the concentration of Ca(OH)<sub>2</sub> varied from 0.01 to 0.07 mol/L.

The metal ion concentration was determined by ICP-OES using an Optima 7000 system (Perkin Elmer, America). The morphology and the composition of the precipitates were examined by scanning electron microscopy (SEM) and energy dispersive spectrometer (EDS) using a Quanta FFG650 system (FEI, America).

### 2.3. Comprehensive separation of metals in tungsten-containing polymetallic solution

According to the components of typical tungsten-containing waste summarized in Table 1, considering that the main metal is W, a high content of Mo, a proper content of Si and a relatively low content of Al and V are chosen to prepare mixed simulation solutions for the multiple metal separation study. The metal concentrations were [WO<sub>3</sub>] = 35 g/L, [MoO<sub>3</sub>] = 10 g/L, [SiO<sub>2</sub>] = 2g/L, [Al<sub>2</sub>O<sub>3</sub>] = 0.175 g/L and [NaVO<sub>3</sub>] = 0.21 g/L. The design of comprehensive separation of W, Mo, V, Si and Al is presented in Fig. 1. MgSO<sub>4</sub>, Fe<sub>2</sub>(SO<sub>4</sub>)<sub>3</sub> and FeSO<sub>4</sub> were used to separate Si and Al, V and W step by step.

The effect of different conditions on each step of the separation was studied through orthogonal experiments. The orthogonal experiments of 4 factors and 4 levels were designed according to Table 2. The factors

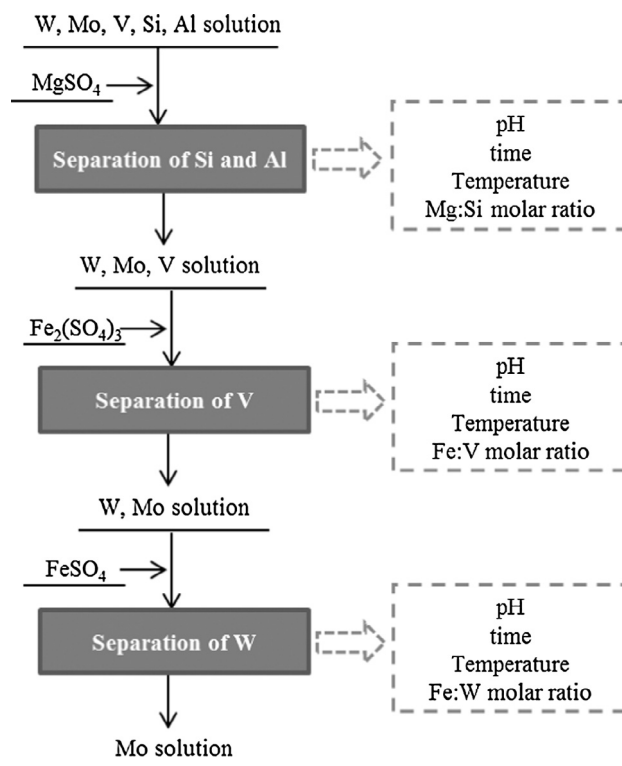


Fig. 1. Comprehensive separation of W, Mo, V, Si and Al.

**Table 2**  
Orthogonal design for 4 factors and 4 levels experiments.

No.	A	B	C	D
1	1	1	1	1
2	1	2	2	2
3	1	3	3	3
4	1	4	4	4
5	2	1	2	3
6	2	2	1	4
7	2	3	4	1
8	2	4	3	2
9	3	1	3	4
10	3	2	4	3
11	3	3	1	2
12	3	4	2	1
13	4	1	4	2
14	4	2	3	1
15	4	3	2	4
16	4	4	1	3

and levels of orthogonal experiments for the separation of Si and Al by magnesium salt are A(1, 2, 3, 4) = pH (7, 8, 9, 10); B(1, 2, 3, 4) = time (min) (10, 30, 50, 70); C(1, 2, 3, 4) = Temperature(°C) (25, 50, 60, 80); D(1, 2, 3, 4) = Mg:Si(1, 1.4, 1.6, 1.8).

The filtrate of experiment No. 11 was utilized to undergo the next separation experiment. Taking into account that the calcium salt would lead to the co-precipitation of W and Mo, the ferric sulfate was selected as a precipitant to react with the V only. The factors and levels of orthogonal experiments for the separation of V are A(1, 2, 3, 4) = pH (7, 8, 9, 10); B(1, 2, 3, 4) = time(min) (10, 30, 50, 70); C(1, 2, 3, 4) = Temperature(°C) (10, 30, 50, 70); D(1, 2, 3, 4) = Fe:V(1, 2, 3, 4).

The filtrate of experiment No. 11 was utilized to undergo the next separation experiment. The ferrous sulfate was selected as a precipitant to separate W from Mo. The factors and levels of orthogonal experiments for the separation of W are A(1, 2, 3, 4) = pH (7, 8, 9, 10); B(1, 2, 3, 4) = time(min) (10, 30, 50, 70); C(1, 2, 3, 4) = Temperature(°C) (20, 30, 40, 50); D(1, 2, 3, 4) = Fe:W(1, 1.2, 1.4, 1.6).

### 3. Results and discussion

#### 3.1. Metal separation of W-Mg-Si-H<sub>2</sub>O system

The E-pH diagrams of the W-Mg-Si-H<sub>2</sub>O system are presented in Fig. 2. Fig. 2(a) indicates the E-pH relationship of the W species in the system; (b) indicates the Mg species; and (c) Si species. As it could be observed from Fig. 2(a), the W precipitated at pH < 5.5 as H<sub>2</sub>WO<sub>4</sub>; being in the ionic state at pH > 11; the magnesium salt could form a compound of MgWO<sub>4</sub> with W, but it was soluble. So W was soluble at pH 5.5–14. From Fig. 2(b), Mg was soluble at pH < 8. If pH > 8, precipitates of 3MgO·4SiO<sub>2</sub>·H<sub>2</sub>O, 3MgO·2SiO<sub>2</sub>·2H<sub>2</sub>O and Mg(OH)<sub>2</sub> formed successively. It was known from Fig. 2(c) that the Si was hydrolyzed at pH ≤ 6.5 to form the colloidal silicic acid H<sub>4</sub>SiO<sub>4</sub>. When the pH was in the range of 6.5–13.5, the SiO<sub>3</sub><sup>2-</sup> formed the precipitates of 3MgO·4SiO<sub>2</sub>·H<sub>2</sub>O and 3MgO·2SiO<sub>2</sub>·2H<sub>2</sub>O with the Mg<sup>2+</sup>. SiO<sub>3</sub><sup>2-</sup> could form a soluble complex of SiO<sub>3</sub><sup>2-</sup>(OH<sup>-</sup>) with OH<sup>-</sup> at pH ≥ 13.5. In order to separate W and Si, two ways existed: firstly, direct regulate pH of W-Si-H<sub>2</sub>O system to 6–8 to make the Si change into colloidal silica and the W into ions; secondly, utilize the magnesium salt in W-Si-H<sub>2</sub>O system to make the Si precipitate with Mg in the pH 8–13.5, whereas the W was in the ionic state. The first method easily produced colloidal silicic acid which was difficult to filtrate, consequently increasing the loss of W, whereas the pH was not easy to control to avoid the W precipitation. Therefore, the second method is better.

The experimental study was conducted for the metal separation of the W-Mg-Si-H<sub>2</sub>O system. The magnesium salt was added to the mixed clarified tungsten salt and silicic acid solution, where consequently the white precipitate appeared. Fig. 3 presents the effects of pH and

reaction duration on the precipitation rate of Si. It was discovered that the precipitation rate of Si had not increased significantly as the pH increased in the range of pH 7–9, whereas the maximum precipitation rate exceeded 99% at pH 9. The Si precipitation mechanism by magnesium salt was as follows: As the pH increased, the single silicate of H<sub>4</sub>SiO<sub>4</sub> was firstly generated. The silicon atom in the H<sub>4</sub>SiO<sub>4</sub> molecule had not yet hexacoordinated and had a polymerization trend. According to the rules of Fajans, the solid particles with high dispersion preferentially adsorbed H<sup>+</sup> to form positive sols. Consequently, the H<sub>4</sub>SiO<sub>4</sub> did not react with Mg<sup>2+</sup>, it was polymerized. As the pH increased, the concentration of H<sub>4</sub>SiO<sub>4</sub> decreased and the polymerization rate of silicic acid decreased. The silicon atoms were in the oxygen tetrahedron, whereas the silicon atoms on the surface of the silicic colloid did not fit the tetrahedral coordination. Consequently, the surface was negatively charged. At this time frame, the Mg<sup>2+</sup> entered the electric double layer of the H<sub>2</sub>SiO<sub>4</sub><sup>2-</sup> colloid to form insoluble particles of MgSiO<sub>3</sub> with the polymerization of the silicate anion, further polymerized with the single silicate to form the high hydrous magnesium silicate (MgO·mSiO<sub>x</sub>·nH<sub>2</sub>O) [22]. When pH = 10, the precipitation rate of Si decreased. This occurred because the magnesium silicate could be decomposed by alkali into magnesium hydroxide and soluble silicate ions at high pH. In contrast, the Si precipitation rate still remained over 90% at pH 10. This meant that the formation reaction of magnesium hydroxide was not dominant. Fig. 4 presents the effects of pH and reaction duration on the precipitation rate of W. It was discovered that the precipitation rate of W decreased gradually with time. This occurred because the magnesium silicate formation was colloidal, which would cause a certain amount of W loss by the corresponding adsorption. As the time passed, the precipitate reaction was complete and the soluble W in the colloid slowly desorbed into the solution. Therefore, the loss of W decreased with time. From the aforementioned analysis, it could be observed that the optimum pH was 9, the reaction duration was 3 h, the precipitation rate of Si was 99% and the W precipitation rate was 2.4%. After precipitation, excessive Mg<sup>2+</sup> and WO<sub>4</sub><sup>2-</sup> coexisted in solution. W would precipitate as tungstic acid when adjusting pH to acidic range (e.g. pH < 2), and separate with Mg in the following process if required.

The precipitate of W-Mg-Si-H<sub>2</sub>O system under the optimum separation conditions was analyzed by SEM and EDS, and the results are shown in Fig. 5. The precipitate presented an inhomogeneous blocky morphology. The EDS was used to preliminarily determine the content of elements of the precipitates as an aid to prove the effect of precipitation. The EDS analysis revealed that the main elements of the precipitate were O, Si and Mg. The precipitate contains no W but amounts of Si and Mg, which agreed well with the precipitation data and demonstrated the effective separation between Si and W.

#### 3.2. Metal separation of W-Al-H<sub>2</sub>O system

The E-pH diagrams of the W-Al-H<sub>2</sub>O system are presented in Fig. 6. Fig. 6(a) indicates the E-pH relationship of the W species in the system; and (b) indicates the Al species. The W did not react with Al to produce precipitates, as presented in Fig. 6(a). The W existed in the H<sub>2</sub>WO<sub>4</sub> precipitate at pH < 6; as well as in the forms of HW<sub>6</sub>O<sub>21</sub><sup>5-</sup> and WO<sub>4</sub><sup>2-</sup> at pH > 6. It could be observed from Fig. 6(b) that the presence of soluble Al species in the solution consisted of the Al(OH)<sub>4</sub><sup>-</sup> and Al<sup>3+</sup>. The Al(OH)<sub>3</sub> precipitated at the pH range of 4.5–10, whereas the Al existed in the ionic state out of this pH range. When pH > 10.5, the Al in solution was almost in the form of Al(OH)<sub>4</sub><sup>-</sup>. Although when pH > 11, the Al(OH)<sub>4</sub><sup>-</sup> and WO<sub>4</sub><sup>2-</sup> might be separated by the solvent extraction, due to the different ion charge, radius, ionic potential and bonding strength to the extractant [23]. This method proved relatively inconvenient. It was discovered from the aforementioned analysis that the Al(OH)<sub>3</sub> could precipitate out of the HW<sub>6</sub>O<sub>21</sub><sup>5-</sup> at 6 < pH < 8. Therefore, it was easier to separate the W and Al through selective precipitation.

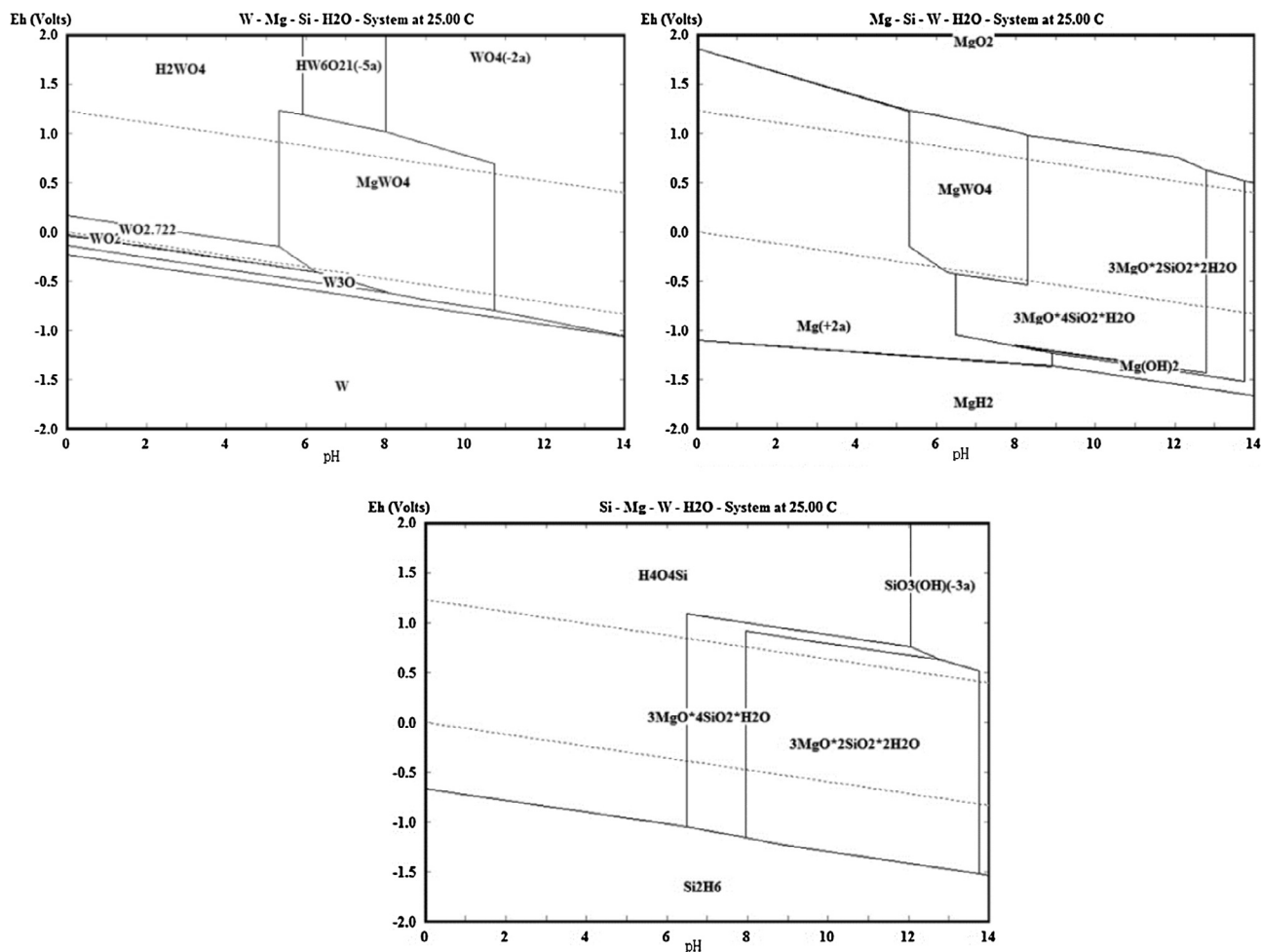


Fig. 2. E-pH diagram of W-Mg-Si-H<sub>2</sub>O system (a) W species; (b) Mg species; (c) Si species.

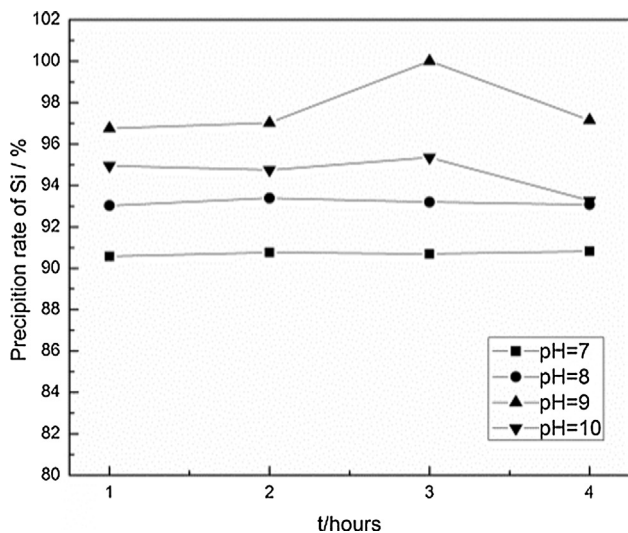


Fig. 3. Effect of pH on Si precipitation in W-Mg-Si-H<sub>2</sub>O system.

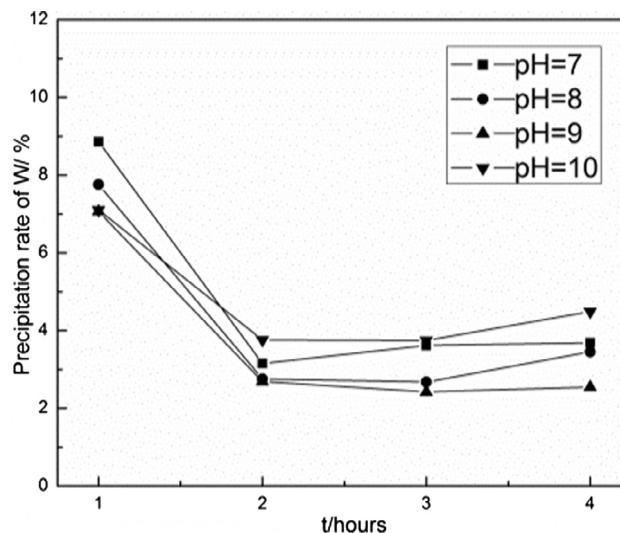


Fig. 4. Effect of pH on W precipitation in W-Mg-Si-H<sub>2</sub>O system.

The experimental study was conducted for the metal separation of the W-Al-H<sub>2</sub>O system. The pH was adjusted for the mixed clarified tungsten salt and aluminum salt solution, where consequently the white precipitate appeared. Figs. 7 and 8 present the effects of pH and reaction duration on the experimental rate of the precipitation of Al and W. From Figs. 7 and 8, it was understood that the Al was substantially

completely precipitated at pH = 7–8, whereas the loss of W was basically below 5.4%. At pH 6, the precipitation rate of Al decreased with time, whereas the loss of W decreased. This occurred because at pH 7–8, the Al was mainly insoluble Al(OH)<sub>3</sub>. Therefore, the precipitation of Al in this pH range could be up to 100%, while the precipitation of W was as low as 2.9%. The Al appeared predominantly soluble Al(OH)<sub>2</sub><sup>+</sup> at pH

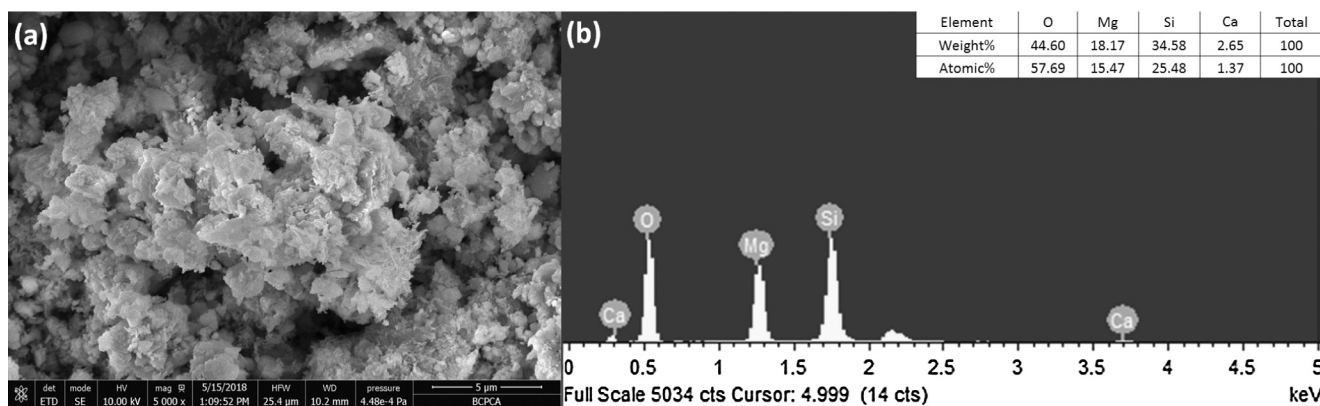


Fig. 5. Precipitate of W-Mg-Si-H<sub>2</sub>O system (a) SEM and (b) EDS.

6. Therefore, the Al precipitation rate decreased, which was unfavorable to the separation of W and Al. The reduction of Al(OH)<sub>3</sub> was beneficial to the reduction of W adsorption. Consequently the precipitation of W in the solution increased gradually with time. The optimum pH was 7, the reaction time was 2 h, the precipitation rate of Al was 99.8% and the W was 3.0%. After precipitation, excessive Al<sup>3+</sup> and WO<sub>4</sub><sup>2-</sup> coexisted in solution. W would precipitate as tungstic acid when adjusting pH to acidic range (e.g. pH < 2), and separate with Al in the following process if required.

The precipitate of W-Al-H<sub>2</sub>O system under the optimum separation conditions was analyzed by SEM and EDS, and the results are shown in Fig. 9. The precipitate presented a loose and irregular blocky morphology. The EDS analysis revealed that the main elements of the precipitate were O, Al and C, and the precipitation contained no W, which agreed well with the precipitation data and demonstrated the effective separation between Al and W.

### 3.3. Metal separation of W-Fe-Mo-H<sub>2</sub>O system

The E-pH diagrams of the W-Fe-Mo-H<sub>2</sub>O system are presented in Fig. 10. Fig. 10(a) indicates the E-pH relationship of the W species in the system; (b) indicates the Fe species; and (c) Mo species. It was discovered in Fig. 10(a) and (b) that the WO<sub>4</sub><sup>2-</sup> could form FeWO<sub>4</sub> with Fe<sup>2+</sup> in the range of 1 ≤ pH ≤ 13. From Fig. 10(c), the Mo could exist as Mo<sub>7</sub>O<sub>24</sub><sup>6-</sup> and MoO<sub>4</sub><sup>2-</sup> at pH > 5.5. According to the differences between the E-pH diagrams, it might be possible to separate W and Mo by the iron salt at 6 ≤ pH ≤ 13. When pH ≥ 13, the FeWO<sub>4</sub> would be decomposed by alkali and the W would be re-dissolved, whereas the Mo was in the form of MoO<sub>4</sub><sup>2-</sup> in the solution. Consequently, it was

impossible to separate W and Mo by the iron salt at pH ≥ 13. The separation pH of W and Mo should be controlled at the pH values of 6–13.

The ferrous sulfate was added to the mixed clarified tungsten and molybdenum salts solution, whereas the dark brown precipitate emerged. Figs. 11 and 12 present the effects of pH and reaction duration on the precipitation of W and Mo. As the reaction duration increased, the precipitation of W and Mo tended to be stable at each pH values. As the pH increase, the precipitation of W decreased and the precipitation of Mo increased, indicating that a low pH was favorable for the separation of W and Mo. At pH 7, the maximum precipitation rate of W was 95% and the lowest loss of Mo was 24%. From the E-pH diagram of the W-Fe-Mo-H<sub>2</sub>O system, the iron salt did not form a compound with Mo. The loss of Mo should be due to the fact that the ferric salt was easily oxidized, forming the Fe(OH)<sub>3</sub> flocculent precipitate, which had a certain adsorption effect on both W and Mo [16]. The higher pH induced the higher amount of the Fe(OH)<sub>3</sub> precipitate and increased the adsorption loss of Mo also. Therefore, in order to effectively separate W and Mo, the pH value of the solution should be set in the range of neutral or weakly alkaline. The optimum pH was 7, the reaction duration was 5 h. Zhongwei Zhao also selected iron or manganese salts for the selective separation of W and Mo. Researches demonstrated that the iron or manganese salts could quite easily precipitate the W than the Mo. Different divalent cations displayed different precipitation ability to the W and Mo. The Ba<sup>2+</sup>, Sr<sup>2+</sup>, Pb<sup>2+</sup>, Ca<sup>2+</sup> and Cd<sup>2+</sup> with low cation force parameter  $\gamma_{orb}^{n+}$  exhibited a low separation coefficient of W and Mo; also, the Mn<sup>2+</sup>, Fe<sup>2+</sup>, Co<sup>2+</sup>, Ni<sup>2+</sup> and Zn<sup>2+</sup> with high cation force parameter  $\gamma_{orb}^{n+}$  exhibited high separation coefficient of W and Mo [15]. In addition, the guanidine nitrate was also utilized to precipitate paratungstate, due to the

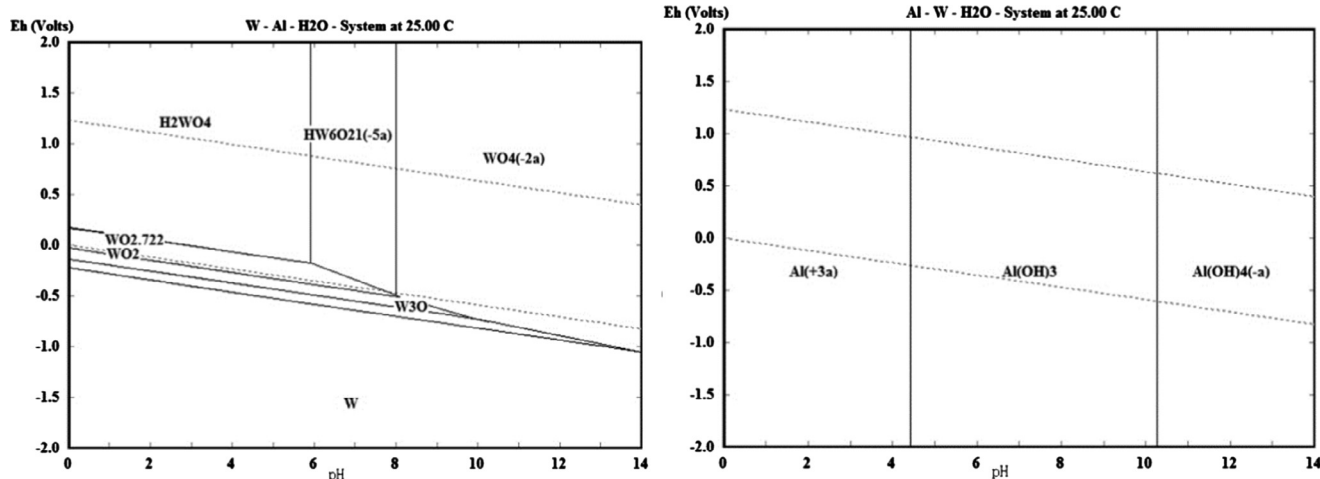


Fig. 6. E-pH diagram of W-Al-H<sub>2</sub>O system (a) W species; (b) Al species.

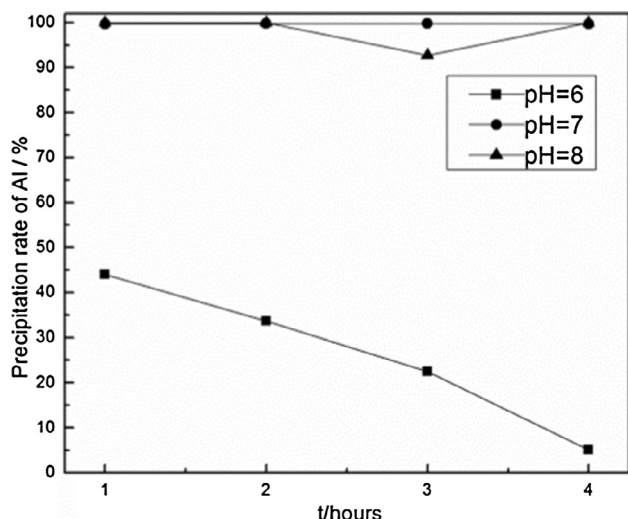


Fig. 7. Effect of pH on Al precipitation in W-Al-H<sub>2</sub>O system.

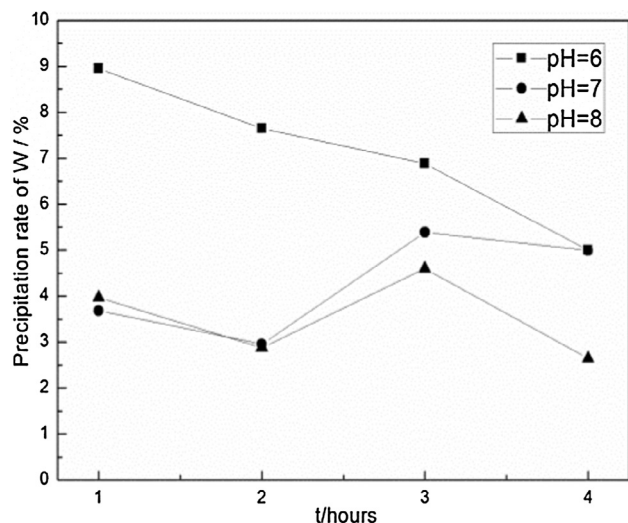


Fig. 8. Effect of pH on W precipitation in W-Al-H<sub>2</sub>O system.

differences in polymerization abilities of W and Mo at pH = 7–8, while the Mo was in the form of MoO<sub>4</sub><sup>2-</sup>, which did not react with the guanidine nitrate [24]. After precipitation in the W-Fe-Mo-H<sub>2</sub>O system, excessive Fe<sup>2+</sup> and MoO<sub>4</sub><sup>2-</sup> coexisted in solution. Fe would precipitate as Fe(OH)<sub>2</sub> when adjusting pH to alkaline range (e.g. pH < 8), and separate with Mo in the following step if required.

Separation of W and Mo has always been a difficult task. The

precipitation method studied in this paper is suitable for recovery of intermediate products or primary products. It has the advantages of simple process and easy to realize batch industrialization. If the high purity of products is required, the solvent extraction should be carried out later.

The precipitate of W-Fe-Mo-H<sub>2</sub>O system under the optimum separation conditions was analyzed by SEM and EDS, and the results are shown in Fig. 13. The precipitate presented small uniform particle morphology. The EDS analysis revealed that the main elements of the precipitate were O, C, Fe, W and Mo, and the atomic ratio of W and Mo was about 2.7. These ratios were close to the precipitation results: the precipitation rate of W was of 95% and Mo of 24%, atomic ratio of W and Mo as 2.1. These results indicated a certain extent of separation between W and Mo.

### 3.4. Metal separation of W-Ca-V-H<sub>2</sub>O system

The ferric iron can form a precipitate with V, which could be utilized as the precipitant for the separation of W and V. If the concentration of V was high in solution, an increased amount of the Fe<sup>3+</sup> precipitant was required, possibly resulting into the formation of an iron hydroxyl colloid, which would adsorb W and increase the W loss, hinder the separation of W and V. Consequently, the calcium salt was selected to precipitate V in the W-Ca-V-H<sub>2</sub>O system (C<sub>NaVO<sub>3</sub></sub> = 0.01 mol/L). The calcium salt was added to the mixed clarified tungsten salt and vanadium salt solution, where consequently the white precipitate appeared. The E-pH diagrams of the W-Ca-V-H<sub>2</sub>O system are presented in Fig. 14. Fig. 14(a) indicates the E-pH relationship of the W species in the system; (b) indicates the Ca species; and (c) V species. According to Fig. 14(a) and (c), W was precipitated as tungstic acid at pH < 2.5 and V was mainly in the form of V<sup>3+</sup>, VO<sup>2+</sup>, VO<sub>2</sub><sup>2+</sup> and HV<sub>10</sub>O<sub>28</sub><sup>5-</sup> at pH < 10, which was beneficial for the separation of W and V. On the other hand, W would form the CaWO<sub>4</sub> with Ca at 2.5 < pH < 16, while V was aggregated into polyatomic isopoly-acids at 2 < pH < 10, which was also favorable for the separation of W and V. As the pH increased, the CaWO<sub>4</sub> was converted into WO<sub>4</sub><sup>2-</sup> at pH > 16.5, whereas the V would form Ca<sub>2</sub>V<sub>2</sub>O<sub>7</sub> and Ca<sub>3</sub>(VO<sub>4</sub>)<sub>2</sub> with Ca at 10 < pH < 17, which was conducive to the separation of W and V at pH > 16.5. According to Fig. 14(b), if the pH value was extremely high, the Ca<sub>2</sub>V<sub>2</sub>O<sub>7</sub> and the Ca<sub>3</sub>(VO<sub>4</sub>)<sub>2</sub> might change into the Ca(OH)<sub>2</sub> precipitate which was unfavorable to the W and V separation. The use of calcium salts for the precipitation separation of W and V is in strong alkaline environment (theoretically pH > 16).

Osseo-Asare [25] studied the E-pH diagram of W-Ca-H<sub>2</sub>O and suggested that precipitation occurred as Ca(OH)<sub>2</sub> rather than as CaWO<sub>4</sub> when adjusting the Ca and W concentrations over pH 13. Kim [26] proposed that V precipitated before the precipitation of W because of a faster response of V than W in W-Ca-V-H<sub>2</sub>O system. This indicates that in fact in the W-Ca-V-H<sub>2</sub>O system, Ca(OH)<sub>2</sub>, Ca<sub>2</sub>V<sub>2</sub>O<sub>7</sub> and Ca<sub>3</sub>(VO<sub>4</sub>)<sub>2</sub>

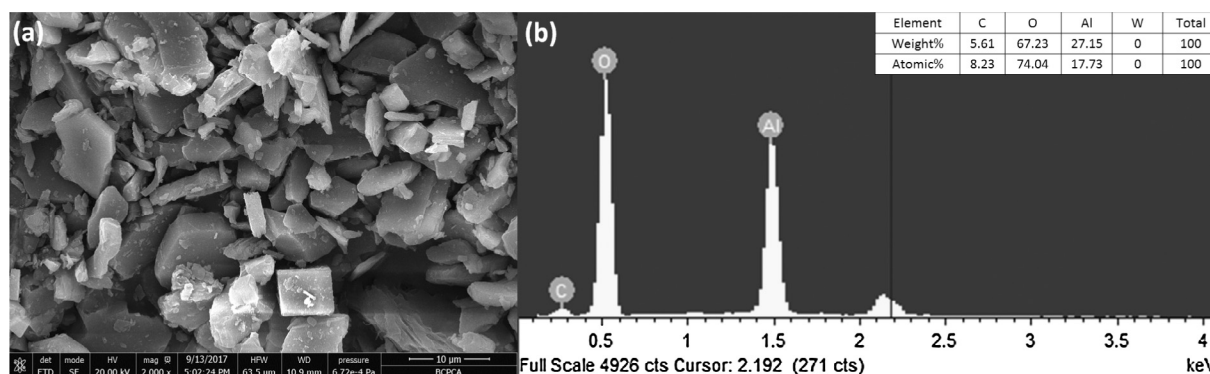


Fig. 9. Precipitate of W-Al-H<sub>2</sub>O (a) SEM and (b) EDS.

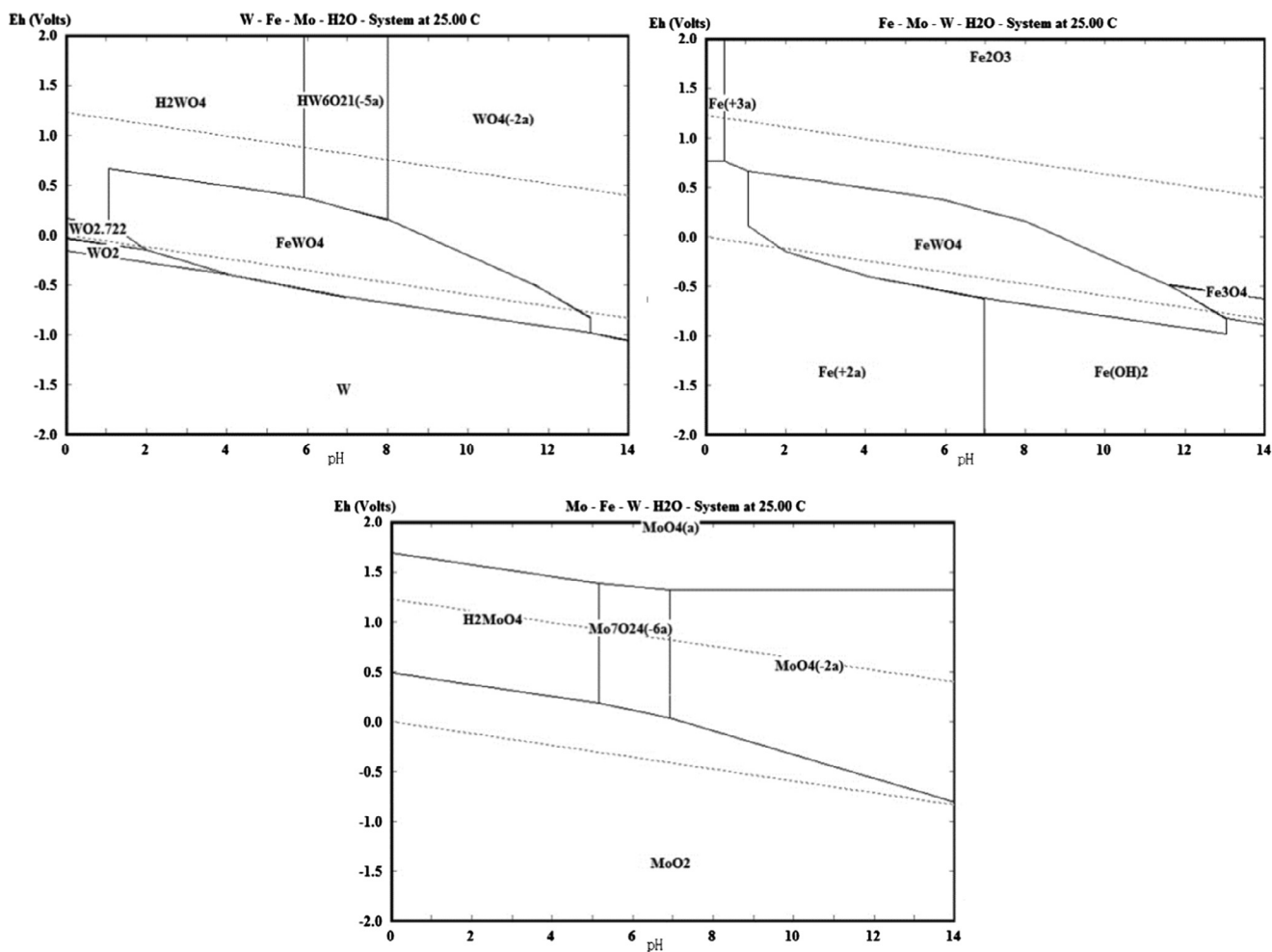


Fig. 10. E-pH diagram of W-Fe-Mo-H<sub>2</sub>O system (a) W species; (b) Fe species; (c) Mo species.

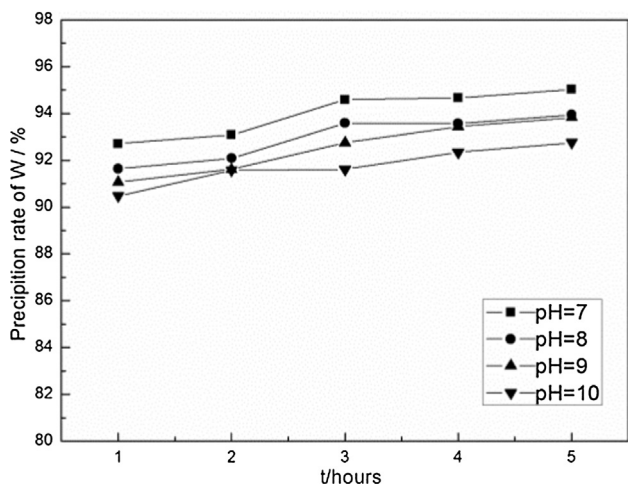


Fig. 11. Effect of pH on W precipitation in W-Fe-Mo-H<sub>2</sub>O system.

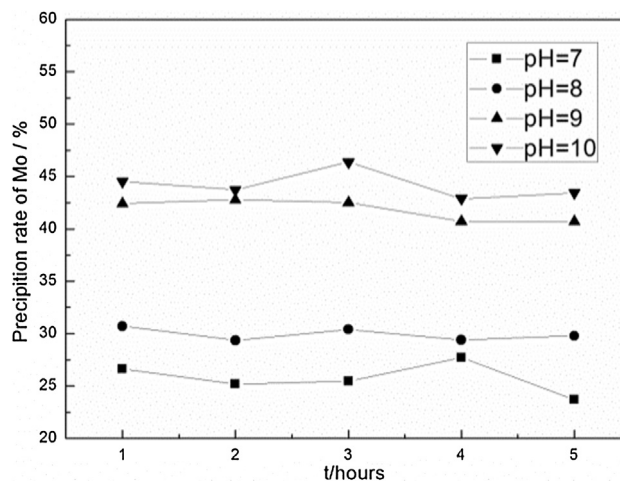


Fig. 12. Effect of pH on Mo precipitation in W-Fe-Mo-H<sub>2</sub>O system.

may preferably emerge rather than CaWO<sub>4</sub> at pH > 13. The effects of reaction duration and molar ratio of Ca:V on the precipitation of W and V at pH 13 are presented in Figs. 15 and 16. Fig. 15 demonstrates that as the reaction duration increased, the precipitation rates of W and V increased slowly, reaching stability at 2 h. The maximum precipitation rate of V reached 70% and the lowest loss of W was 0.1% at 4 h. Fig. 16 demonstrates that when Ca:V ≤ 3, the precipitation rate of V gradually increased; when Ca:V ≥ 3, the V precipitation rate remained stable. The

V precipitation rate reached 91.2% and the W loss was 4.3% at Ca:V = 3. The experimental results demonstrated that the separation of W and V by calcium hydroxide was feasible. The validity of this method has also been proved by literature [26]: 98.6% of V and 7.7% of W precipitated out when Ca(OH)<sub>2</sub> were performed. After precipitation, excessive Ca<sup>2+</sup> and WO<sub>4</sub><sup>2-</sup> coexisted in solution. W would precipitate as primary product of CaWO<sub>4</sub> when adjusting pH to alkaline range as about 10; or W would form tungstic acid to separate with Ca<sup>2+</sup> when

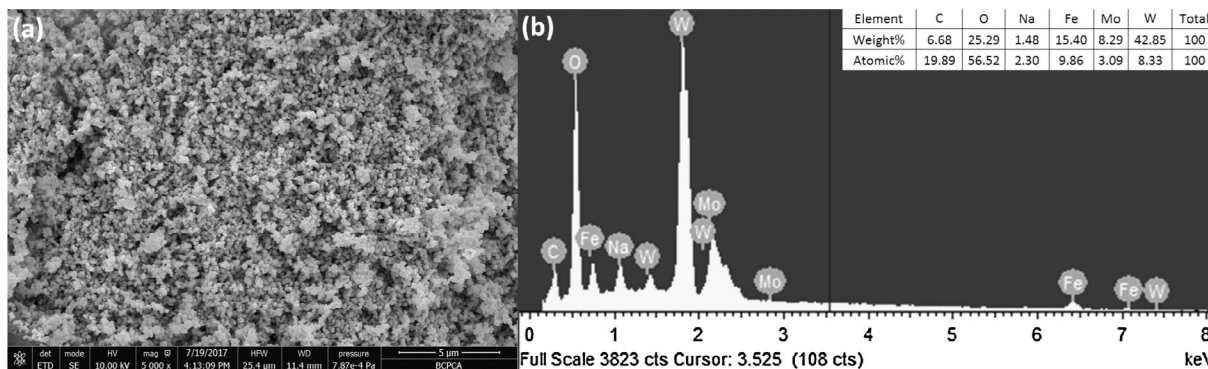


Fig. 13. Precipitate of W-Fe-Mo-H<sub>2</sub>O (a) SEM and (b) EDS.

adjusting pH to about 2 in the following step if required.

The precipitate of W-Ca-V-H<sub>2</sub>O system obtained under the optimum separation conditions was characterized by SEM and EDS, shown in Fig. 17. The precipitate presented irregular lamellar morphology. The EDS analysis revealed that the main elements of the precipitate were O, Ca, V and small amounts of W. The atomic ratio of V and W in precipitate was about 33.5. Although this ratio was lower than the precipitation results, the preferential precipitation of V over W was clearly proved. It was effective and feasible to separate V and W by calcium salt.

3.5. Comprehensive separation of metals in tungsten-containing polymetallic solutions

According to the components of typical tungsten-containing waste, separation of W, V, Mo, Al and Si is one of the core aspects of the recovery process for tungsten secondary resources. The polymetallic solution of W, Mo, V, Si and Al was prepared for the orthogonal multiple metal separation study, according to Fig. 1. MgSO<sub>4</sub> was used to separate Si and Al. Figs. 18–21 present the effects of pH, time, temperature and molar ratio of Mg:Si on the metal precipitation rates of W, Mo, V, Si and Al, respectively. Each data constituted the average values

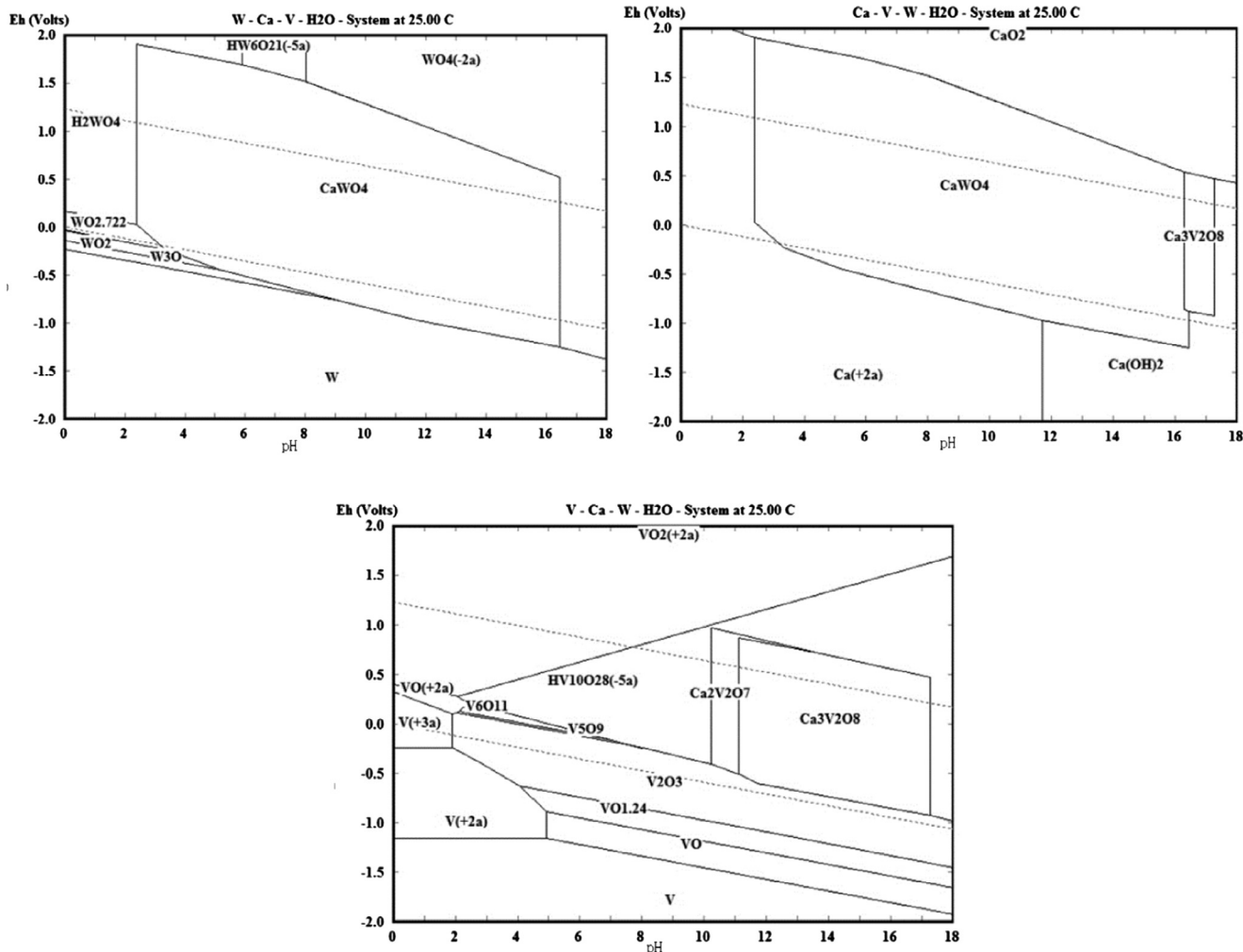


Fig. 14. E-pH diagram of W-Ca-V-H<sub>2</sub>O system (a) W species; (b) Ca species; (c) V species.

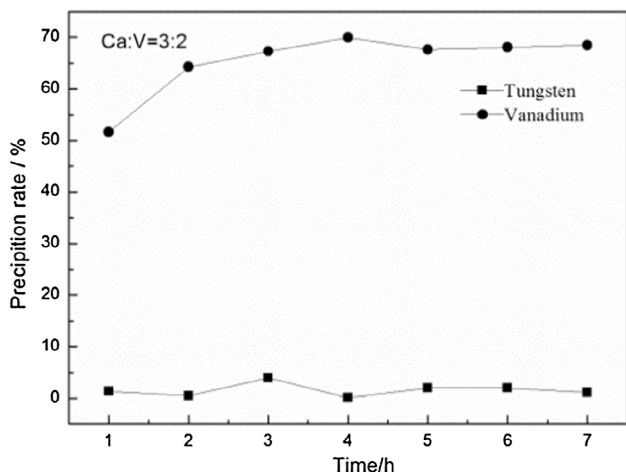


Fig. 15. Effects of reaction duration on precipitation rates of W and V in W-Ca-V-H<sub>2</sub>O system.

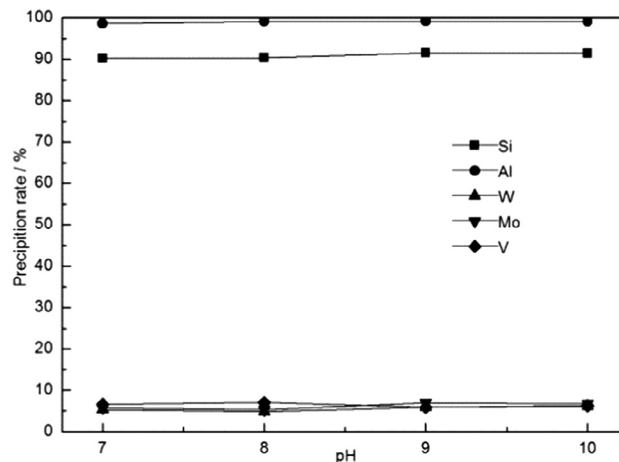


Fig. 18. Effect of pH during separation of Si and Al.

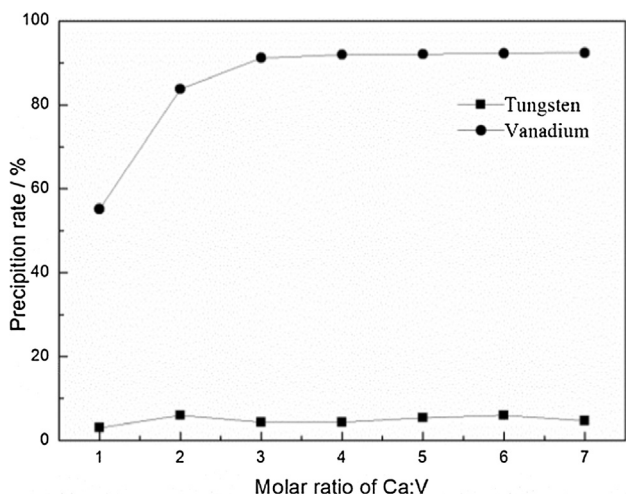


Fig. 16. Effects of different molar ratios on precipitation rates of W and V in W-Ca-V-H<sub>2</sub>O system.

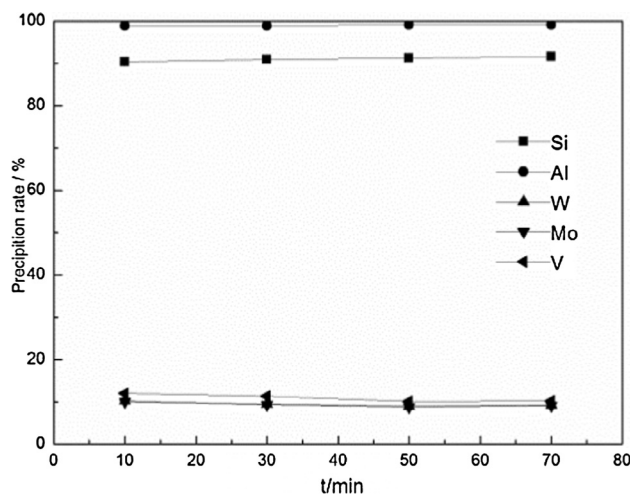


Fig. 19. Effect of time during separation of Si and Al.

for the same factor of different levels. As it could be observed from these figures, the precipitation rates of Si and Al exceeded 90.25% and 98.64% under all conditions, whereas the losses of W, Mo and V were below 13%. The magnesium salt could not only precipitate Si, whereas also it could precipitate Al. This occurred because the process not only produced the magnesium silicate precipitation, whereas it also produced double salt precipitates of Si, Al and Mg. The optimal conditions were pH = 9, 50 min, 50 °C and Mg:Si = 1.4. The desirable value of the

precipitation rates of Si, Al, W, Mo and V would reach approximately 92%, 99%, 4%, 5% and 5%, respectively.

The range analysis of each factor in the separation process of Si and Al is presented in Figs. 22–26. The priority orders of the precipitation factors of Si, Al, W, Mo and V were Mg:Si > pH > t > T, pH > Mg:Si > T > t, Mg:Si > T > t > pH, Mg:Si > T > pH > t and Mg:Si > t > pH > T, respectively.

Fe<sub>2</sub>(SO<sub>4</sub>)<sub>3</sub> was used to separate V. The Fe<sup>3+</sup>, Mn<sup>2+</sup> and Al<sup>3+</sup> in the solution would form corresponding hydroxides under the alkaline conditions, whereas the Fe<sup>3+</sup> and Mn<sup>2+</sup> might produce Fe(VO<sub>3</sub>)<sub>3</sub> and Mn(VO<sub>3</sub>)<sub>2</sub> at approximately pH = 8 with VO<sub>3</sub><sup>-</sup>. Therefore, the Fe<sup>3+</sup>

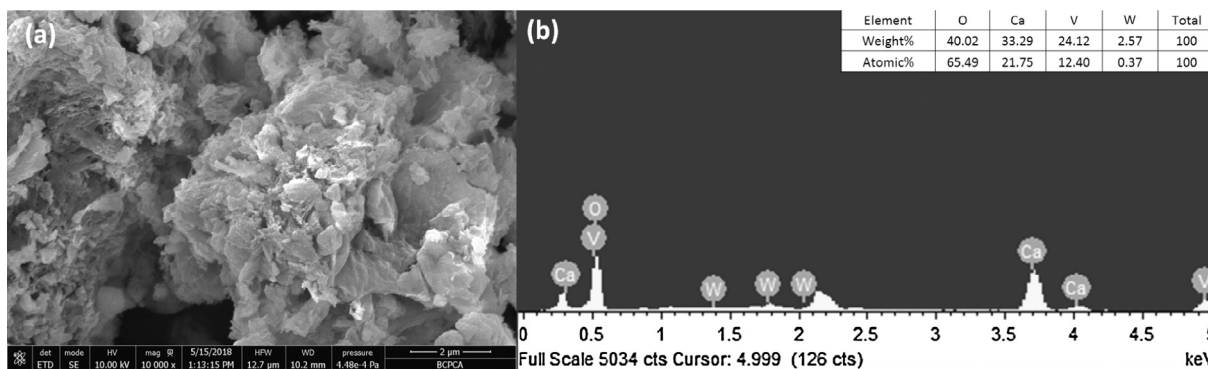


Fig. 17. Precipitate of W-Ca-V-H<sub>2</sub>O (a) SEM and (b) EDS.

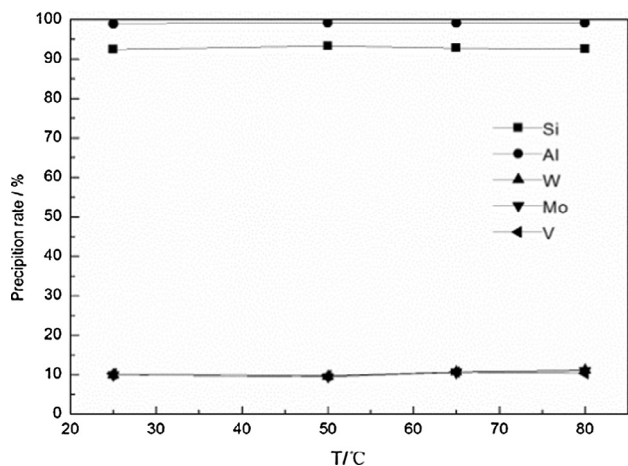


Fig. 20. Effect of temperature during separation of Si and Al.

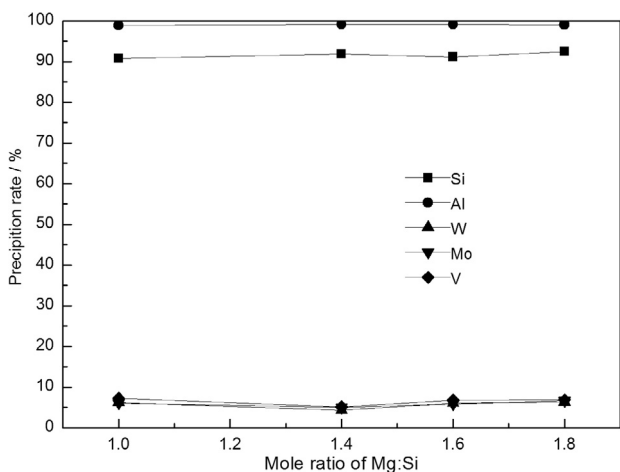


Fig. 21. Effect of mole ratio of Mg:Si during separation of Si and Al.

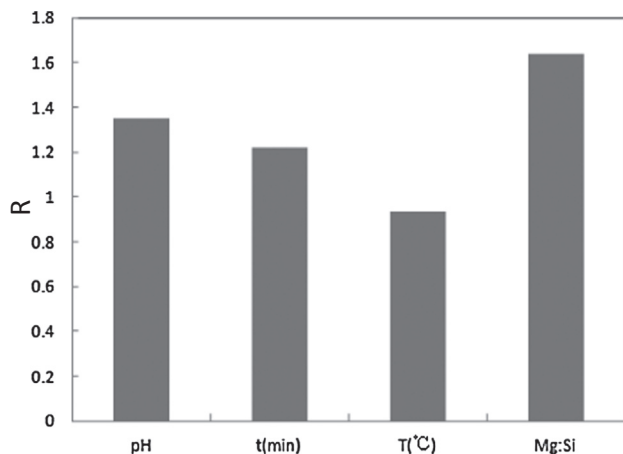


Fig. 22. Range of precipitation of Si during separation of Si and Al.

could be selected to precipitate the V out of W and Mo, especially for the polymetallic solutions with relatively low V concentration in the W-Ca-V-H<sub>2</sub>O system (C<sub>NaVO<sub>3</sub></sub> = 0.0017 mol/L), which would not consume an increased amount of Fe<sup>3+</sup> and produce a high amount of Fe(OH)<sub>3</sub>, reducing the W adsorption loss. In addition, Fe<sup>3+</sup> will not react with W and Mo, unlike Ca<sup>2+</sup> which will cause the coprecipitation of W and Mo [15]. Therefore, the ferric sulfate was selected as the precipitating agent to separate the V. Figs. 27–30 present the effects of pH, time,

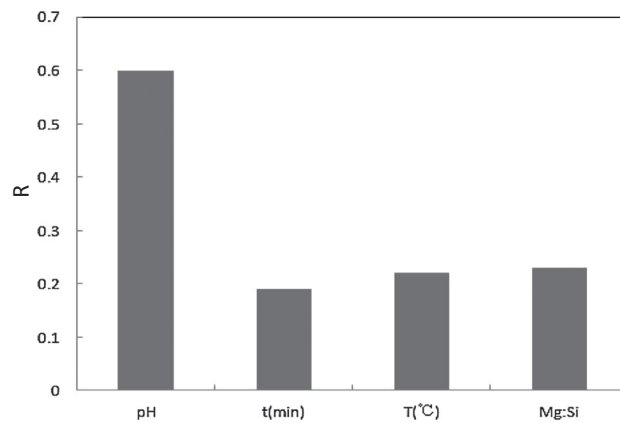


Fig. 23. Range of precipitation of Al during separation of Si and Al.

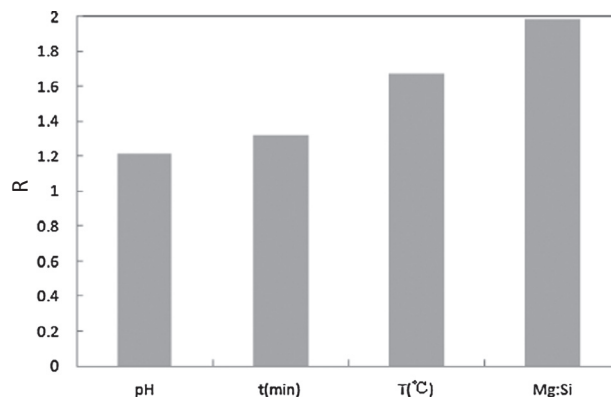


Fig. 24. Range of precipitation of W during separation of Si and Al.

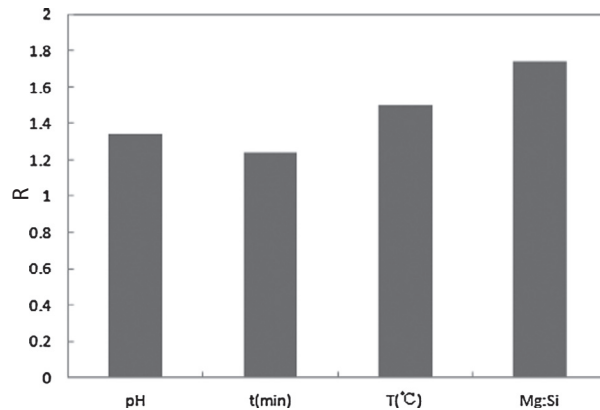


Fig. 25. Range of precipitation of Mo during separation of Si and Al.

temperature and molar ratio of Fe:V on the precipitation rates of W, Mo and V. Each data constituted the average value for the same factor of different levels. The separation effect of ferric sulfate was good and the V precipitation rate exceeded 94.97%, whereas the losses of W and Mo were relatively low, with the lowest precipitation rates of 2.62% and 1.56%, respectively. The optimal conditions were pH = 9, t = 50 min, T = 70 °C and Fe:V = 2. The desirable value of the precipitation rates of V, W and Mo would reach approximately 96%, 3% and 2%, respectively. The precipitation mechanism was that the V had stronger polymerization ability than the W, when the pH was at 8.5–9.0. Most vanadium ions were in main polymerization states of H<sub>2</sub>V<sub>10</sub>O<sub>28</sub><sup>4-</sup>, V<sub>4</sub>O<sub>12</sub><sup>4-</sup> and V<sub>5</sub>O<sub>15</sub><sup>5-</sup>, however, the W was almost entirely converted in the form of WO<sub>4</sub><sup>2-</sup>. The polymeric vanadium ions had lower valence than the WO<sub>4</sub><sup>2-</sup> ions, so they had stronger affinity to high valence ions,

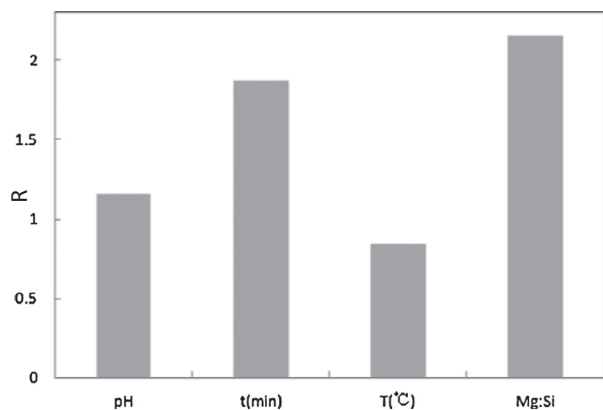


Fig. 26. Range of precipitation of V during separation of Si and Al.

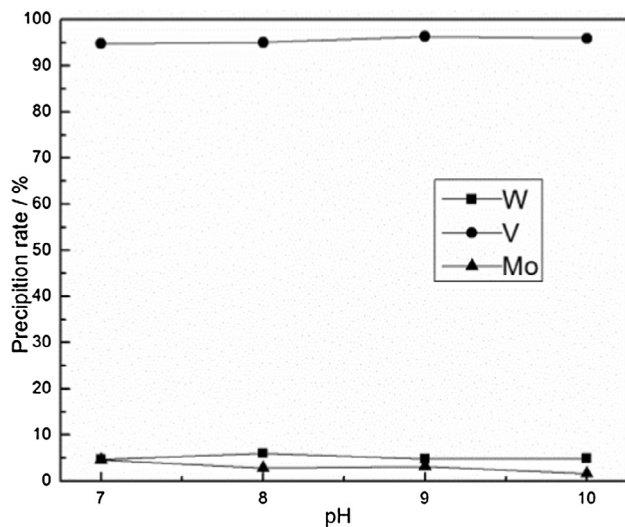


Fig. 27. Effect of pH during separation of V.

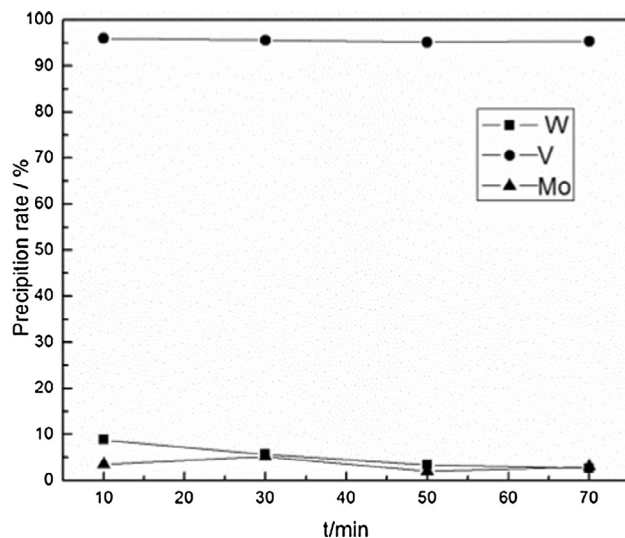
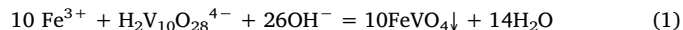


Fig. 28. Effect of time during separation of V.

such as  $\text{Fe}^{3+}$ , which could be considered essentially as a weak alkaline anion exchange agent. Therefore, the  $\text{Fe}^{3+}$  can be preferentially adsorbed via electrostatic force and then precipitated at the pH of 8.5–9.0 by the  $\text{H}_2\text{V}_{10}\text{O}_{28}^{4-}$ ,  $\text{V}_4\text{O}_{12}^{4-}$  and  $\text{V}_5\text{O}_{15}^{5-}$ , promoting the separation of W and V [24,27]. The reaction of  $\text{H}_2\text{V}_{10}\text{O}_{28}^{4-}$  and  $\text{Fe}^{3+}$  is presented in

formula (1):



The range analysis of each factor in the separation process of V is presented in Figs. 31–33. The priority orders of the precipitation factors of V, W and Mo were  $T > \text{pH} > t > \text{Fe:V}$ ,  $t > T > \text{Fe:V} > \text{pH}$  and  $t > T > \text{pH} > \text{Fe:V}$ , respectively.

$\text{FeSO}_4$  was used to separate W. The ferrous sulfate was utilized to separate the W and Mo. Figs. 34–37 present the effects of pH, time, temperature and molar ratio of Fe:W on the precipitation rates of W and Mo. Each data constituted the average value for the same factor of different levels. The precipitation rate of W was relatively high, basically beyond 91%, whereas the Mo loss was also significant, the maximum could reach to 47.36% and the minimum was 21.1%. The separation of W and Mo is always difficult as they are similar in nature. The optimal conditions were  $\text{pH} = 8$ ,  $t = 30 \text{ min}$ ,  $T = 30^\circ\text{C}$  and  $\text{Fe:W} = 1.2$ . The desirable value of the precipitation rates of W and Mo would reach approximately 97% and 29%, respectively.

The range analysis of each factor in the separation process of W is presented in Figs. 38–39. The priority orders of the precipitation factors of W and Mo were  $\text{Fe:W} > T > t > \text{pH}$  and  $\text{Fe:W} > \text{pH} > T > t$ , respectively.

According to the above orthogonal experimental results, under the optimum condition, Si could be separated with the estimated precipitation rate of 92% and the most important factor affecting precipitation is Mg:Si; Al could be separated with the estimated precipitation rate of 99% and the most important factor affecting precipitation is pH; V could be separated with the estimated precipitation rate of 96% and the most important factors affecting precipitation is T; W could be separated with the estimated precipitation rate of 97% and the most important factors affecting precipitation is Fe:W.

As W recovery rate was 96%, 97.38%, 97%; Mo was 95%, 98.44%, 71% in the first, the second and the third step of the comprehensive separation process, respectively, the W total recovery rate =  $96\% \times 97.38\% \times 97\% = 90.68\%$  and the Mo total recovery rate =  $95\% \times 98.44\% \times 71\% = 66.39\%$ . The ion concentration of the final solution could be estimated based on the initial concentration and precipitation rate of the relevant elements if necessary. Further recovery of W from the precipitate which contains Mo could be carried out by means of extraction and ion exchange.

#### 4. Conclusions

- (1) The E-pH diagrams of the tungsten-containing systems, such as the W-Mg-Si-H<sub>2</sub>O, the W-Al-H<sub>2</sub>O, the W-Fe-Mo-H<sub>2</sub>O and the W-Ca-V-H<sub>2</sub>O, were plotted. The metal precipitation separation properties were studied through theoretical and experimental analysis. The results demonstrated that Si could precipitate with Mg to separate with ionic W at the pH 8–13.5 theoretically in the W-Mg-Si-H<sub>2</sub>O system, whereas the optimal experimental separation rate of Si was 99% with the W loss of 2.4% at pH 9.  $\text{Al}(\text{OH})_3$  could precipitate out of the  $\text{HW}_6\text{O}_{21}^{5-}$  at  $6 < \text{pH} < 8$  theoretically in the W-Al-H<sub>2</sub>O system, whereas the optimal experimental separation rate of Al was 99.8% with the W loss of 3.0% at pH 7. W could be separated with Mo by the ferrous salt at pH 6–13 theoretically in the W-Fe-Mo-H<sub>2</sub>O system, whereas the optimal experimental separation rate of W was 95% with the Mo loss of 24% at pH = 7. V could be separated with W by calcium salts in strong alkaline environment theoretically in the W-Ca-V-H<sub>2</sub>O system, whereas the optimal experimental separation rate of V was 91.2% with the W loss of 4.3% at pH 13. The theoretical predictions and experimental results were basically in agreement.
- (2) The comprehensive separation process for tungsten-containing polymetallic solution of W, Mo, V, Si and Al was designed and the

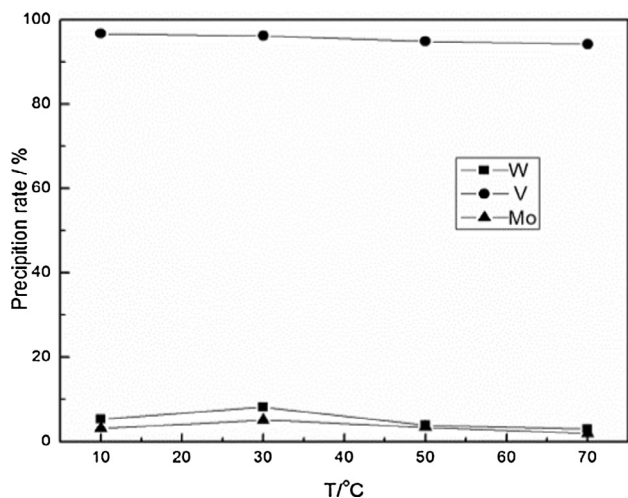


Fig. 29. Effect of temperature during separation of V.

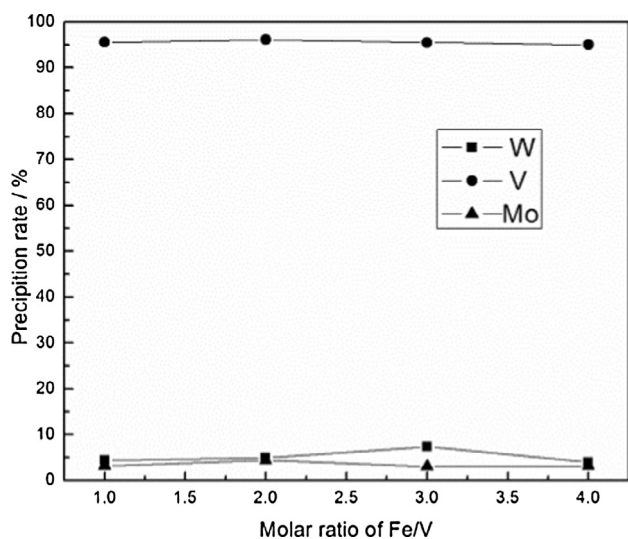


Fig. 30. Effect of mole ratio of Fe:V during separation of V.

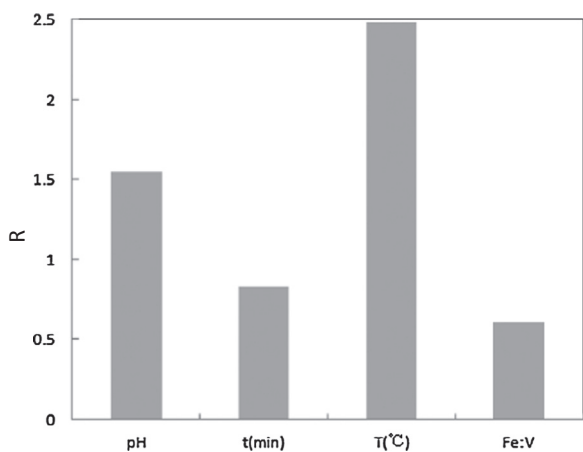


Fig. 31. Range of precipitation of V during separation of V.

parameters were optimized through the orthogonal method. The optimal conditions for the separation of Si and Al by the magnesium sulfate were pH = 9, 50 min, 50 °C and Mg:Si = 1.4, with the desirable value of the precipitation rates of Si, Al, W, Mo and V approximately 92%, 99%, 4%, 5% and 5%. The optimal conditions for

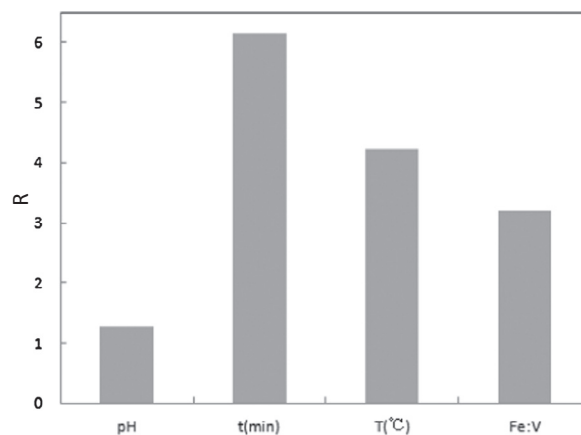


Fig. 32. Range of precipitation of W during separation of V.

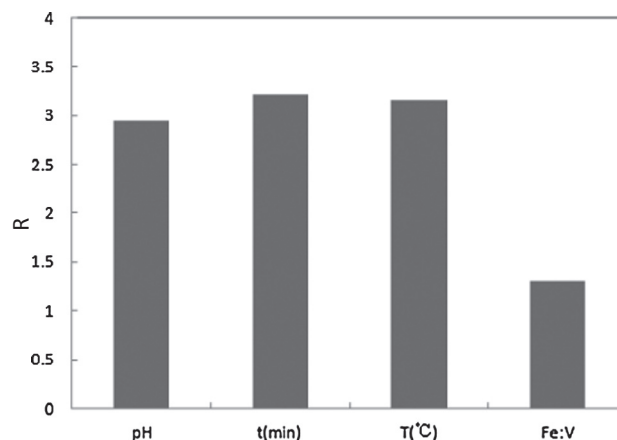


Fig. 33. Range of precipitation of Mo during separation of V.

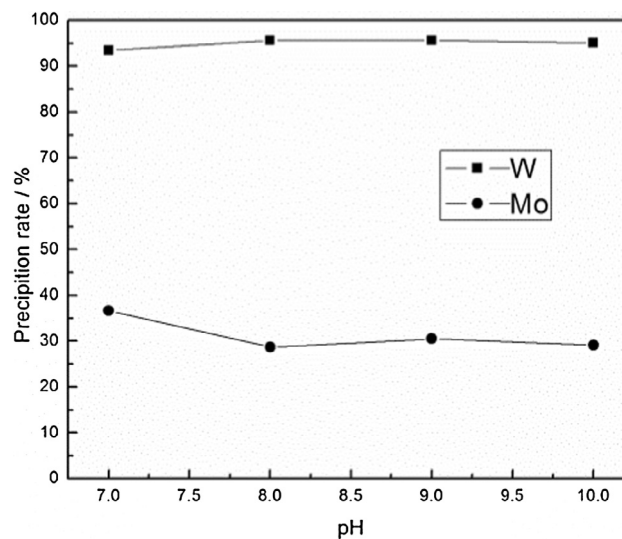


Fig. 34. Effect of pH during separation of W.

the separation of V by ferric sulfate were pH = 9, t = 50 min, T = 70 °C and Fe:V = 2, with the desirable value of the precipitation rates of V, W and Mo approximately 96%, 3% and 2%. The optimal conditions for the separation of W and Mo by ferrous sulfate were pH = 8, t = 30 min, T = 30 °C and Fe:W = 1.2, with the desirable value of the precipitation rates of W and Mo approximately 97% and 29%. The W total recovery rate was 90.68%. The comprehensive separation processes could selectively precipitate

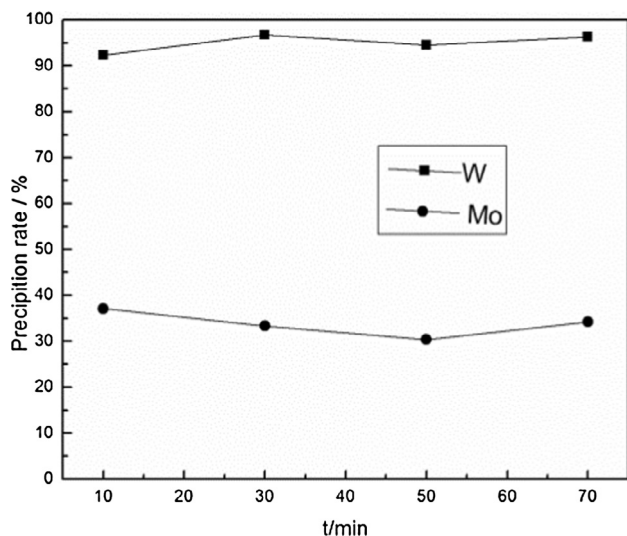


Fig. 35. Effect of time during separation of W.

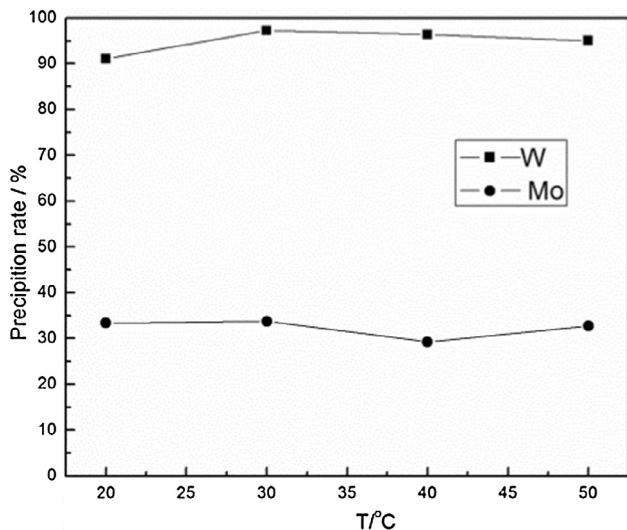


Fig. 36. Effect of temperature during separation of W.

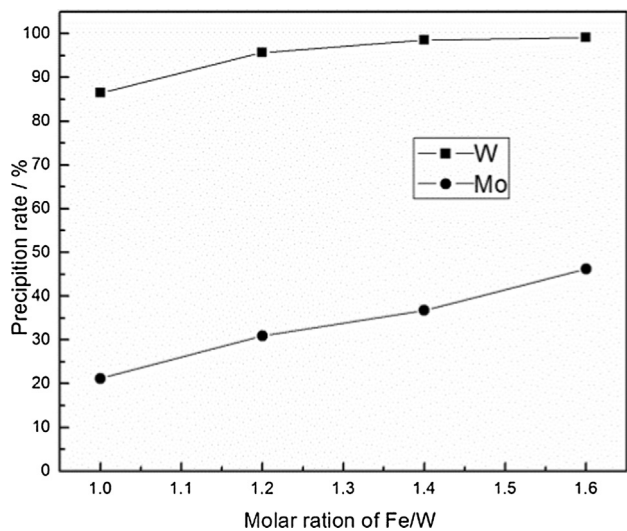


Fig. 37. Effect of mole ratio of Fe:W during separation of W.

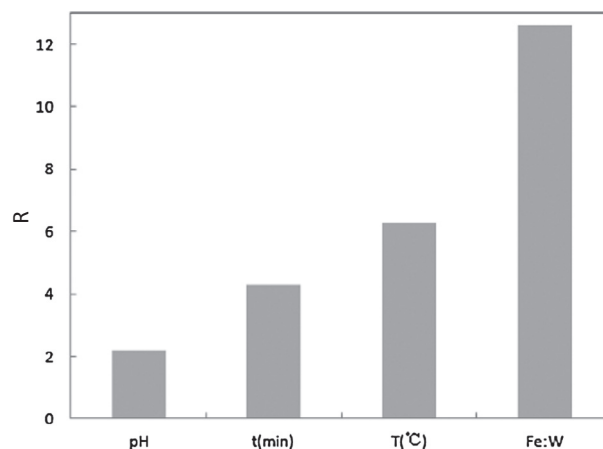


Fig. 38. Range of precipitation of W during separation of W.

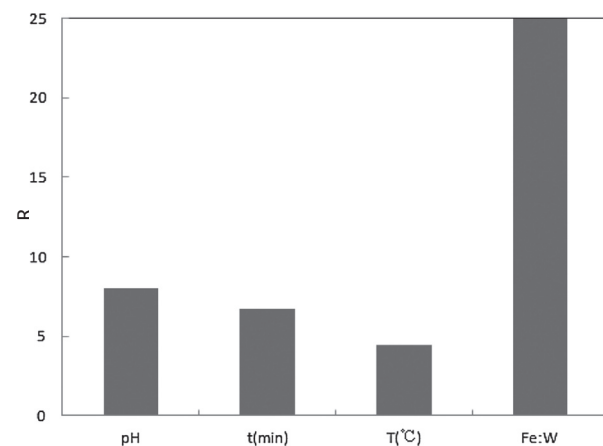


Fig. 39. Range of precipitation of Mo during separation of W.

and separate metals, providing reference for the recovery of tungsten secondary resources.

**Acknowledgements**

This work was supported by National Natural Science Foundation of China (51621003, 51422401, 51304010), Science and Technology Project of Beijing Municipal Education Commission (KM201810005009), Beijing Municipal Natural Science Foundation (2172010) and the Construction Project for National Engineering Laboratory for Industrial Big-data Application Technology (312000522303).

**Appendix A. Supplementary material**

Supplementary data associated with this article can be found, in the online version, at <https://doi.org/10.1016/j.seppur.2018.07.013>.

**References**

- [1] D.R. Leal-Ayala, J.M. Allwood, E. Petavratzi, T.J. Brown, G. Gunn, Mapping the global flow of tungsten to identify key material efficiency and supply security opportunities, *Resour. Conserv. Recycl.* 103 (2015) 19–28.
- [2] N. Strigul, A. Koutsospyros, P. Arienti, C. Christodoulatos, D. Dermatas, W. Braidia, Effects of tungsten on environmental systems, *Chemosphere* 61 (2005) 248–258.
- [3] A.D. Koutsospyros, N. Strigul, W. Braidia, C. Christodoulatos, Tungsten: environmental pollution and health effects, *Encyclopedia Environ. Health* (2011) 418–426.
- [4] P. Sun, H. Li, Y. Li, M. Liu, P. Su, Study on treatment of ammonia leaching slag in the metallurgical process of tungsten, *J. Central South Univ. Technol.* 2 (2) (1995) 21–26.
- [5] I.H. Choi, H.R. Kim, G. Moon, R.K. Jyothi, J.Y. Lee, Spent V<sub>2</sub>O<sub>5</sub>-WO<sub>3</sub>/TiO<sub>2</sub> catalyst

- processing for valuable metals by soda roasting-water leaching, *Hydrometallurgy* 175 (2018) 292–299.
- [6] L. Luo, L.K. Jun, A. Shibayama, Recovery of tungsten and vanadium from tungsten alloy scrap, *Hydrometallurgy* 72 (2004) 1–8.
- [7] S. Hairunnisha, G.K. Sendil, J.P. Rethinaraj, G.N. Srinivasan, P. Adaikkalam, S. Kulandaisamy, Studies on the preparation of pure ammonium paratungstate from tungsten alloy scrap, *Hydrometallurgy* 85 (2007) 67–71.
- [8] L. Luo, T. Miyazaki, A. Shibayama, W. Yen, T. Fujita, A novel process for recovery of tungsten and vanadium from a leach solution of tungsten alloy scrap, *Miner. Eng.* 16 (2003) 665–670.
- [9] Z.X. Lin, L.H. Liu, Q. Lin, Y.L. Ye, Recovery of tungsten and cobalt from wasted tungsten carbide, *Chin. J. Process Eng.* 9 (2009) 93–96.
- [10] J.I. Martins, J.L. Lima, A. Moreira, S.C. Costa, Tungsten recovery from alkaline leach solutions as synthetic scheelite, *Hydrometallurgy* 85 (2007) 110–115.
- [11] L. Zhang, Z. Nie, X. Xi, L. Ma, Electrochemical separation and extraction of cobalt and tungsten from cemented scrap, *Sep. Purif. Technol.* 195 (2018) 244–252.
- [12] C. Edtmaier, R. Schiesser, C. Meissl, Selective removal of the cobalt binder in WC/Co based hardmetal scraps by acetic acid leaching, *Hydrometallurgy* 76 (1) (2005) 63–71.
- [13] T. Kojima, T. Shimizu, R. Sasai, H. Itoh, Recycling process of WC-Co cermets by hydrothermal treatment, *J. Mater. Sci.* 40 (19) (2005) 5167–5172.
- [14] J. Lee, E. Kim, J. Kim, W. Kim, B. Kim, B.D. Pandey, Recycling of WC–Co hardmetal sludge by a new hydrometallurgical route, *J. Refract. Metals Hard Mater.* 29 (2011) 365–371.
- [15] Z.W. Zhao, C.F. Cao, X.Y. Chen, G.S. Huo, Separation of macro amounts of tungsten and molybdenum by selective precipitation, *Hydrometallurgy* 108 (2011) 229–232.
- [16] Z.W. Zhao, C.F. Cao, X.Y. Chen, Separation of macro amounts of tungsten and molybdenum by precipitation with ferrous salt, *Trans. Nonferrous Metals Soc. China* 21 (2011) 2758–2763.
- [17] C.F. Cao, Z.W. Zhao, X.Y. Chen, Selective precipitation of tungstate from molybdate-containing solution using divalent ions, *Hydrometallurgy* 110 (2011) 115–119.
- [18] P. Ning, H. Cao, Y. Zhang, Selective extraction and deep removal of tungsten from sodium molybdate solution by primary amine N1923, *Sep. Purif. Technol.* 70 (2009) 27–33.
- [19] T.H. Nguyen, S.L. Man, Separation of vanadium and tungsten from sodium molybdate solution by solvent extraction, *Ind. Eng. Chem. Res.* 53 (20) (2014) 8608–8614.
- [20] Z.W. Zhao, J.L. Zhang, X.Y. Chen, X.H. Liu, J.T. Li, W.G. Zhang, Separation of tungsten and molybdenum using macroporous resin: equilibrium adsorption for single and binary systems, *Hydrometallurgy* 140 (2013) 120–127.
- [21] P. Zhang, K. Inoue, K. Yoshizuka, H. Tsuyama, Extraction and selective stripping of molybdenum(VI) and vanadium(IV) from sulfuric acid solution containing aluminum(III), cobalt(II), nickel(II) and iron(III) by LIX 63 in Exxsol D80, *Hydrometallurgy* 41 (1) (1996) 45–53.
- [22] L. Feng, M. Li, G.Q. Liu, L. Han, R. Yang, Synthesis of magnesium trisilicate by a reverse strike method and its microscopic analysis, *J. Univ. Sci. Technol. Beijing* 31 (12) (2009) 1600–1604.
- [23] C. Xiao, L. Zeng, J. Wei, L. Xiao, G. Zhang, Thermodynamic analysis for the separation of tungsten and aluminium in alkaline medium using solvent extraction, *Hydrometallurgy* 174 (2017) 91–96.
- [24] J.L. Zhang, Z.W. Zhao, Thermodynamic analysis for separation of tungsten and vanadium in W(VI)-V(V)-H<sub>2</sub>O system, *Chin. J. Nonferrous Metals* 24 (6) (2014) 1656–1662.
- [25] K. Osseo-Asare, Solution chemistry of tungsten leaching systems asare, *Metallurg. Mater. Trans. B* 13 (1982) 555–564.
- [26] J.W. Kim, W.G. Lee, I.S. Hwang, J.Y. Lee, C. Han, Recovery of tungsten from spent selective catalytic reduction catalysts by pressure leaching, *J. Ind. Eng. Chem.* 28 (2015) 73–77.
- [27] Q. Gao, P. Shi, C. Liu, M. Jiang, Experimental study on liquid precipitation of iron vanadate, *J. Northeast. Univ. (Nat. Sci.)* 36 (1) (2015) 33–37.